

1 **SUPPLEMENTARY MATERIAL**

2 **Black Carbon Seasonal and Diurnal Variation in surface snow in Svalbard and its**  
3 **Connections to Atmospheric Variables**

4 Michele Bertò<sup>1#</sup>, David Cappelletti<sup>2,7</sup>, Elena Barbaro<sup>1,3</sup>, Cristiano Varin<sup>1</sup>, Jean-Charles  
5 Gallet<sup>4</sup>, Krzysztof Markowicz<sup>5</sup>, Anna Rozwadowska<sup>6</sup>, Mauro Mazzola<sup>7</sup>, Stefano  
6 Crocchianti<sup>2</sup>, Luisa Poto<sup>1,3</sup>, Paolo Laj<sup>8</sup>, Carlo Barbante<sup>1,3</sup> and Andrea Spolaor<sup>1,2</sup>.

7

8 <sup>1</sup> Ca' Foscari University of Venice, Dept. Environmental Sciences, Informatics and Statistics,  
9 via Torino, 155 - 30172 Venice-Mestre, Italy;

10 <sup>2</sup> Università degli Studi di Perugia, Dipartimento di Chimica, Biologia e Biotecnologie,  
11 Perugia, Italy;

12 <sup>3</sup> CNR-ISP, Institute of Polar Science – National Research Council –via Torino, 155 - 30172  
13 Venice-Mestre, Italy;

14 <sup>4</sup> Norwegian Polar Institute, Tromsø, Norway.

15 <sup>5</sup> University of Warsaw, Institute of Geophysics, Warsaw, Poland;

16 <sup>6</sup> Institute of Oceanology, Polish Academy of Sciences, Sopot, Poland;

17 <sup>7</sup> CNR-ISP, Institute of Polar Science – National Research Council – Via Gobetti 101,  
18 Bologna;

19 <sup>8</sup> Univ. Grenoble-Alpes, CNRS, IRD, Grenoble-INP, IGE, 38000 Grenoble, France

20

21 <sup>#</sup> Now at Laboratory of Atmospheric Chemistry, Paul Scherrer Institute, 5232 Villigen PSI,  
22 Switzerland

23

24

25

26

27

28

29

30

31

32

33

34

## 35 **1. Details of the statistical analyses**

36 The two multiple regression models were fitted on the logarithm scale because the  
37 distribution of rBC concentrations in both the experiments is characterized by a significant  
38 skewness. Coarse mode particles number concentrations and conductivity were also log-  
39 transformed to linearize their relationships with  $\log(\text{rBC})$ . Graphical inspection of residuals  
40 plots and normal probability plots confirmed that after the logarithm transformations, the  
41 regression models meet the assumptions of linearity, constant error variance (called  
42 homoscedasticity in the statistical literature) and normal errors. The regression model fitted  
43 on the 80-days (daily sampling resolution) experiments is:

44

$$45 \log(\text{rBC}) = \beta_0 + \beta_1 \log(\text{dust}) + \beta_2 \text{eBC} + \beta_3 \text{temp} + \beta_4 \text{snow} + \beta_5 \text{SWR} + \beta_6 \log(\text{cond}) + \epsilon$$

46

47 In the regression model ‘dust’ indicates coarse mode particles number concentrations,  
48 ‘temp’ is the snow temperature, ‘snow’ is an indicator for the solid precipitation, ‘SWR’ is  
49 solar incoming shortwave radiation, ‘cond’ is the conductivity and  $\epsilon$  is a normal error. In the  
50 3-days experiment (hourly resolution), the model includes also trigonometric components  
51  $\sin(2\pi \text{hour}/24)$  and  $\cos(2\pi \text{hour}/24)$  to account for the hourly periodicity of the incoming  
52 solar energy. The statistical analyses were performed with the statistical language R (R Core  
53 Team, 2020).

54

## 55 **2. Calibration of the SP2**

56 The empirical calibration of the SP2, performed using size selected fullerene soot particles is  
57 linear up to 500 nm, and the assumption is that it is also linear beyond that size (and the  
58 corresponding mass). However, when a massive particle enters the laser beam the  
59 incandescence signal might saturate the detector; therefore, in this analysis only the particles  
60 below 700 nm were considered. The evaluation of the BC mass for the samples showing a  
61 BC geometric mean mass equivalent diameter above 300/400 nm, might therefore be more  
62 influenced resulting in an underestimation of the mass. However, the evaluation of the  
63 missing mass is beyond the scope of this manuscript and require further analyses. The losses  
64 of mass due to the presence of undetected small particles, below 80/70 nm of MED, is not  
65 significant given that the geometric mean of the MED of the mass size distributions is always  
66 above 150 nm.

67

### 68 **3. Possible interferences during the SP2 rBC mass concentration in Arctic snow**

69 The surface snow of the Svalbard archipelago is normally characterized by high content of  
70 sea salt particles, for example those containing Na, due to its geographical position  
71 surrounded by the ocean. The Na concentration in the samples analyzed in this work is, on  
72 average, about 500 ng g<sup>-1</sup>. We cannot exclude that the rBC mass concentration variability for  
73 the 80-days experiment presented in this work might have been slightly influenced by the Na  
74 content (tracer of sea salt deposition), however any clear relation appeared from the  
75 comparison between the rBC and the Na mass concentrations during the “80 days”  
76 experiment (Fig. SI 3). As a precaution, all samples from the 3-days experiments were diluted  
77 five times with Milli-Q water prior to the SP2 analyses. The SP2 instrumental performances  
78 during the analyses, in terms of laser power and incandescence signal quality, were  
79 monitored and constant. At the best of our knowledge, no study focusing on the possible  
80 effects of the Na particles on the rBC mass concentration retrieved from the SP2 has been  
81 published in the literature. Further analyses of snow samples collected in areas characterized  
82 by a high influence of marine-like aerosols could shed light on the effects of salt particles on  
83 the rBC mass and number concentration via SP2 measurements, as well as establishing a  
84 shared procedure to avoid measuring artifacts.

85 Moreover, mineral dust particles might have an influence on the SP2 measurements,  
86 depending on their chemical and physical properties. Currently, the literature lacks  
87 investigation on these specific SP2-mineral dust particles interactions. However, a few  
88 studies on snow and ice samples measured with an SP2 take the assumptions that mineral  
89 dust particles are not detected by the SP2 as incandescence signals, but only as scattering  
90 signals (Kaspari et al., 2011). Recent studies, based on atmospheric measurements suggest  
91 that the SP2 rBC mass concentration measurement can potentially be interfered by the  
92 presence of metals and metals-oxide (Moteki et al., 2017), of volcanic ashes or of dust  
93 (Kupiszewski et al., 2016).

### 94 **4. Ancillary measurements for the 3-days samples: Na, Mn, EC, OC**

95 Ancillary data were measured/gathered for the 3-days experiment in order to  
96 strengthening the interpretations even though they were not considered in the statistical  
97 exercise. The Mn concentrations are considered to be a good proxy for mineral dust aerosols  
98 (Baker et al., 2006). In **Errore. L'origine riferimento non è stata trovata.** the Mn  
99 concentration profile was compared with that of the coarse mode particles concentration

100 showing a very similar behavior and suggesting a common source. Despite some differences,  
101 a similar pattern is also clearly visible for all the various chemical species.

102         Every six hours a surface snow sample was collected in parallel to that of the hourly  
103 sampling. These samples water volume was of about  $1618 \pm 290 \text{ mL cm}^3$  and they were used  
104 for TC, EC and OC measurement, and the results are shown in Fig. SI 4. A different profile is  
105 shown for the three compounds compared to that of the rBC mass concentration. As reported  
106 above the two measuring techniques are different and, in particular, the size range of particles  
107 detected by the two instruments is different, from 80 to 600 nm for the SP2 whereas a much  
108 broader dimensional spectrum for the Sunset, potentially explaining part of the observed  
109 difference. Interestingly, the EC daily values increased of one order of magnitude, from 1 to  
110  $10 \mu\text{g l}^{-1}$ , during the sampling period, showing a maximum during the precipitation episode.  
111 For more info and results about the comparison between rBC and EC snow/ice measurement  
112 check Sigl et al. (2018). On the contrary, the OC atmospheric concentration showed a  
113 decreasing trend showing the highest values at the beginning of the sampling period and the  
114 lowest at the end, similarly to the atmospheric eBC behavior. Remarkably, the highest OC  
115 concentration was found in the same sample were the highest concentration of all the other  
116 measured compounds was found (at the very beginning of the snow episode) suggesting a  
117 common atmospheric scavenging process (although not above the average for the rBC mass  
118 concentration).

119

120

121

122

123

124

125

126

127

128

129 **Table S1.** Abakus Klotz selected dimensional bins.

Channel	Size ( $\mu\text{m}$ )	11	2.2	22	6.4
1	0.8	12	2.4	23	7.1
2	0.9	13	2.6	24	7.8
3	1	14	2.9	25	8.6
4	1.1	15	3.2	26	9.5
5	1.2	16	3.5	27	10.5
6	1.3	17	3.9	28	11.6
7	1.4	18	4.3	29	12.8
8	1.6	19	4.8	30	14.1
9	1.8	20	5.3	31	15.5
10	2	21	5.8	32	80

130

131

132

133

134

135

136

137

138

139

140

141

142

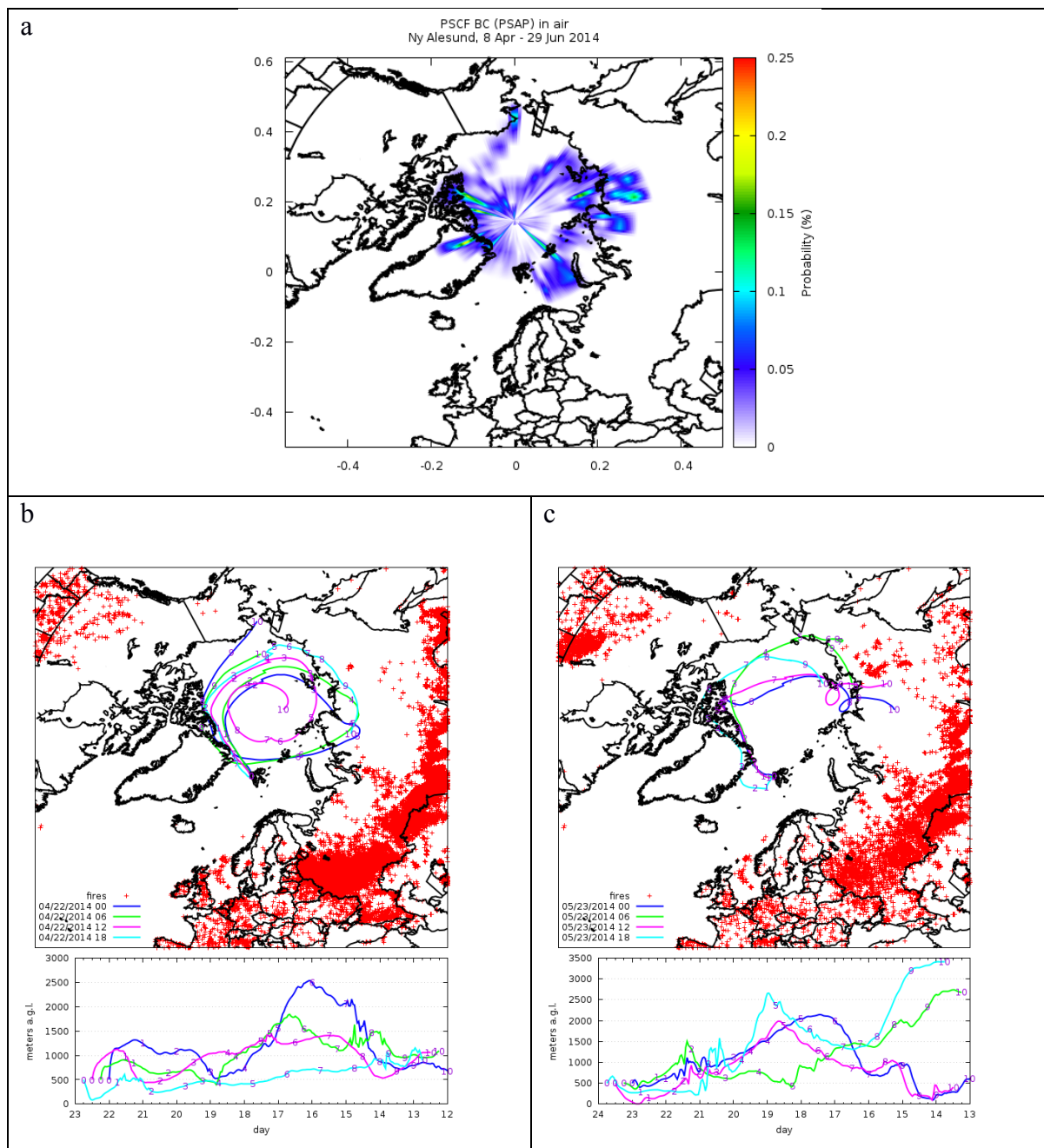
143

144

145

146

147 **Figure S1.** a) Potential source contribution function analysis (PSCF) of eBC recorded in the  
148 80-days experiment (8 April-29 June). 10 days back-trajectories for two selected days: b) 22  
149 April and c) 23 May. Four BTs were calculated for the two selected days, with a 6 hours  
150 interval. The red crosses represent the fires taking place during the last 10 days (data from the  
151 MODIS active fire products (<https://firms.modaps.eosdis.nasa.gov/firemap>)).

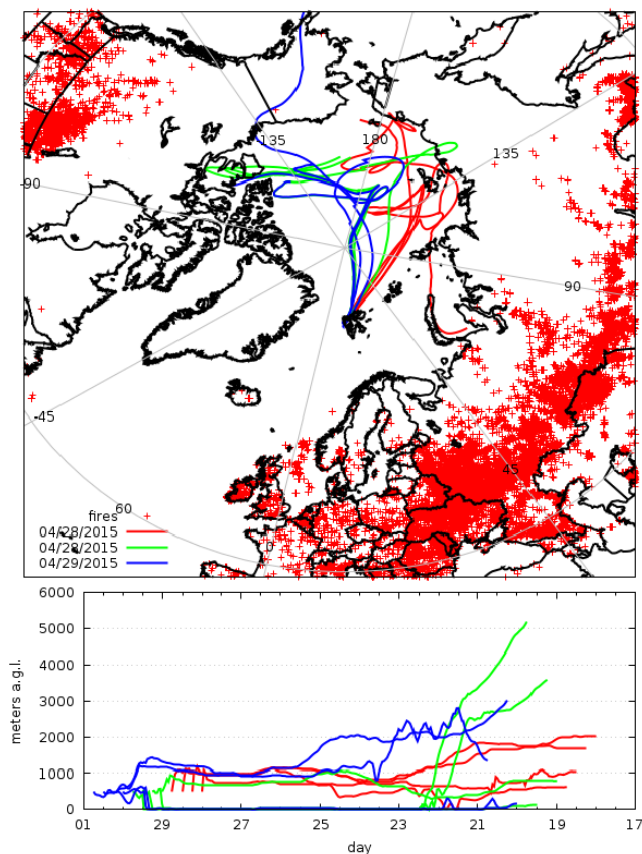


152

153

154

155 **Figure S2.** 10 days back-trajectory results for the 3-days experiment (three per day with a 8  
156 hours interval). The red crosses represent the fires taking place during the last 10 days (data  
157 from the MODIS active fire products (<https://firms.modaps.eosdis.nasa.gov/firemap/>)).



158  
159  
160  
161  
162  
163  
164  
165  
166  
167

168 **Figure S3.** Results for the 80-days experiment from ancillary measurements. Upper panel:  
169 rBC mass concentration (gray line), Na concentration (red line) and conductivity (green line).  
170 Lower panel: atmospheric eBC mass concentration (black line) and ammonia as measured at  
171 the Zeppelin station, Svalbard (gray bars).

172

173

174

175

176

177

178

179

180

181

182

183

184

185

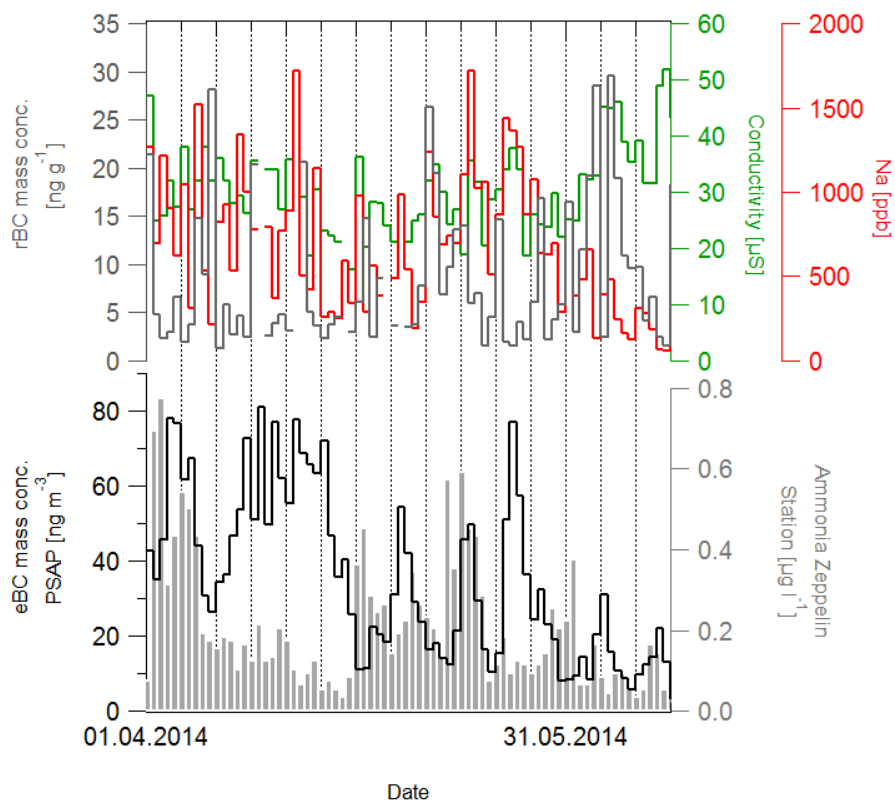
186

187

188

189

190





191 **Figure S4.** The 3-days experiments results from ancillary measurements. Uppermost panel:  
 192 manganese (Mn, dark-yellow line) mass concentration and the coarse mode particles number  
 193 (blu line). Second uppermost panel: rBC mass concentration (gray line) with sodium (Na)  
 194 concentration (red line) and conductivity (green line). Second lowermost panel: atmospheric  
 195 eBC mass concentration (black line), snow OC concentration (blue bars) and daily average of  
 196 atmospheric ammonia as measured at the Zeppelin station (gray bars). Lowermost panel: TC  
 197 (red bars), OC (blue bars) and EC (green bars) and EC daily average (black line).

198

199

200

201

202

203

204

205

206

207

208

209

210

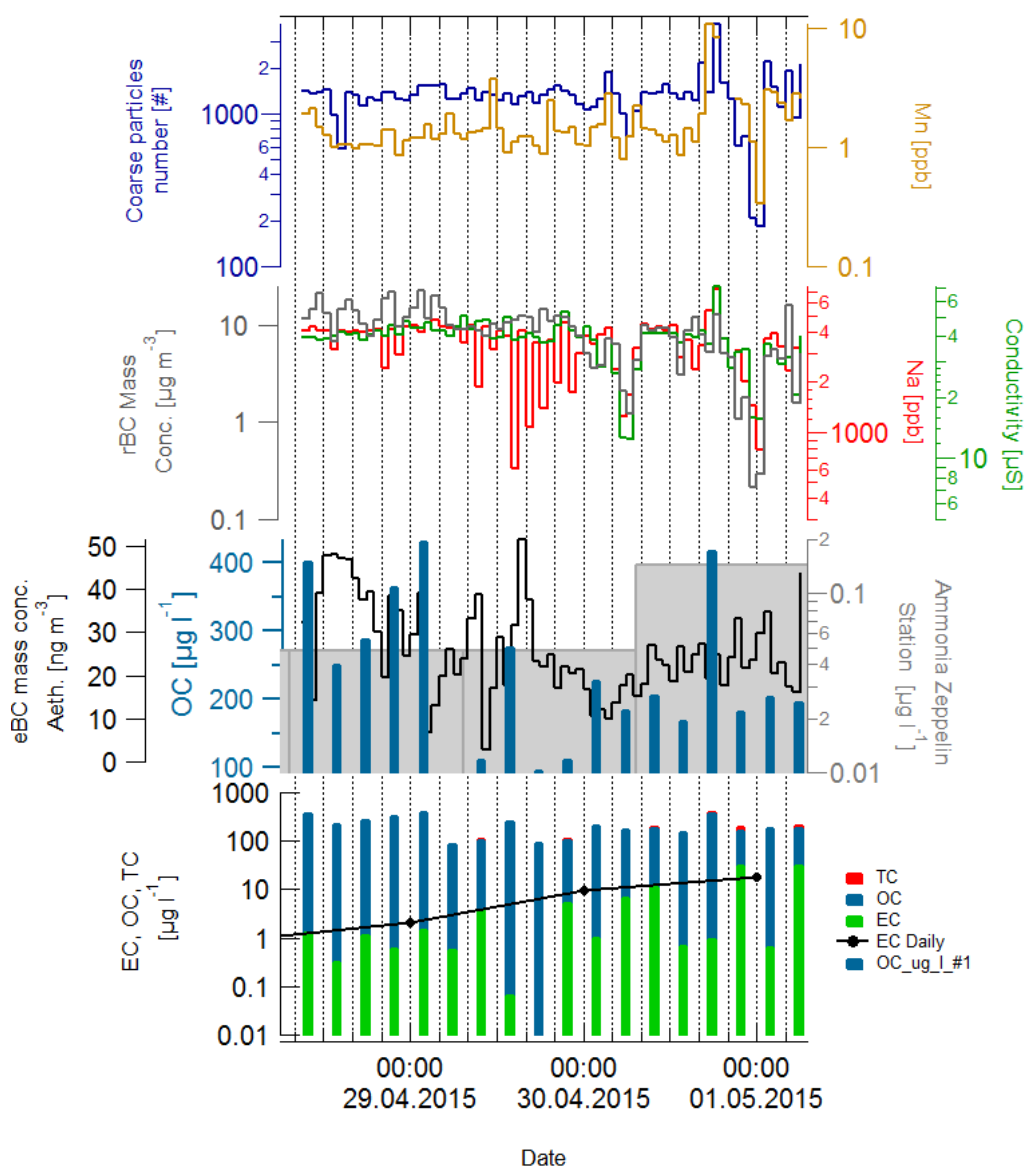
211

212

213

214

215



216 **References:**

- 217 Kaspari, S. D., Schwikowski, M., Gysel, M., Flanner, M. G., Kang, S., Hou, S. and  
218 Mayewski, P. A.: Recent increase in black carbon concentrations from a Mt. Everest ice  
219 core spanning 1860–2000 AD, *Geophysical Research Letters*, 38(4),  
220 doi:10.1029/2010GL046096, 2011.
- 221 Kupiszewski, P., Zanatta, M., Mertes, S., Vochezer, P., Lloyd, G., Schneider, J., Schenk, L.,  
222 Schnaiter, M., Baltensperger, U., Weingartner, E. and Gysel, M.: Ice residual properties in  
223 mixed-phase clouds at the high-alpine Jungfraujoch site, *Journal of Geophysical Research:*  
224 *Atmospheres*, 121(20), 12,343–12,362, doi:10.1002/2016JD024894, 2016.
- 225 Moteki, N., Adachi, K., Ohata, S., Yoshida, A., Harigaya, T., Koike, M. and Kondo, Y.:  
226 Anthropogenic iron oxide aerosols enhance atmospheric heating, *Nature Communications*,  
227 8, 15329, doi:10.1038/ncomms15329, 2017.
- 228 Sigl, M., Abram, N. J., Gabrieli, J., Jenk, T. M., Osmont, D. and Schwikowski, M.: 19th  
229 century glacier retreat in the Alps preceded the emergence of industrial black carbon  
230 deposition on high-alpine glaciers, *The Cryosphere*, 12(10), 3311–3331,  
231 doi:https://doi.org/10.5194/tc-12-3311-2018, 2018.
- 232 R Core Team: R: A language and environment for statistical computing. Vienna, Austria: R  
233 Foundation for Statistical Computing; 2020. URL <https://www.R-project.org>